Modelling the deformation of the elastin network in the aortic valve

Afshin Anssari-Benam * **and Andrea Bucchi**

The BIONEER centre,
Cardiovascular Engineering Research Lab (CERL),
School of Engineering,
University of Portsmouth,
Anglesea Road,
Portsmouth PO1 3DJ
United Kingdom

* Address for correspondence: Afshin Anssari-Benam,
The BIONEER centre,
Cardiovascular Engineering Research Lab (CERL),
School of Engineering,
University of Portsmouth,
Anglesea Road,
Portsmouth PO1 3DJ
United Kingdom

Tel: +44 (0)23 9284 2187
Fax: +44 (0)23 9284 2351
E-mail: afshin.anssari-benam@port.ac.uk

Word count (Introduction to References): 5636

Abstract

This paper is concerned with proposing a suitable structurally-motivated strain energy function, denoted by $W_e^{elastinnetwork}$, for modelling the deformation of the elastin network within the aortic valve (AV) tissue. The AV elastin network is the main non-collagenous load-bearing component of the valve matrix and therefore, in the context of continuum-based modelling of the AV, the $W_e^{elastinnetwork}$ strain energy function would essentially serve to model the contribution of the '*isotropic matrix*'. To date, such a function has mainly been considered as either a generic neo-Hookean term or a general exponential function. In this paper, we take advantage of the established structural analogy between the network of elastin chains and the freely jointed molecular chain networks to customise a structurally-motivated $W_e^{elastinnetwork}$ function on this basis. The ensuing stress-strain (force-stretch) relationships are thus derived and fitted to the experimental data points reported by Vesely (1998) for intact AV elastin network specimens under uniaxial tension. The fitting results are then compared with those of the neo-Hookean and the general exponential models, as the frequently used models in the literature, as well as the *Arruda-Boyce* model as the gold standard of the network chain models. It is shown that our proposed $W_e^{elastinnetwork}$ function, together with the general exponential and the *Arruda-Boyce* models provide excellent fits to the data, with R^2 values in excess of 0.98, while the neo-Hookean function is entirely inadequate for modelling the AV elastin network. However, the general exponential function may not be amenable to rigorous interpretation, as there is no structural meaning attached to the model. It is also shown that the parameters estimated by the *Arruda-Boyce* model are not mathematically and structurally valid, despite providing very good fits. We thus conclude that our proposed strain energy function $W_e^{elastinnetwork}$ is the preferred choice for modelling the behaviour of the AV elastin network and thereby the '*isotropic matrix*'. This function may therefore be superimposed onto that of the anisotropic collagen fibres family in order to develop a structurally-motivated continuum-based model for the AV.

Keywords: Aortic valve, elastin network, strain energy function, continuum-based model, biomechanical behaviour.

Modelling the deformation of the elastin network in the aortic valve

1 Introduction

Within the framework of continuum mechanics, models developed for application to collagenous soft tissues incorporate strain energy functions that account for the contribution of the family of collagen fibres, as well as the '*isotropic matrix*'. The presence of the collagen fibre family (families) dispersed within the '*isotropic matrix*' endows the tissues with a strong anisotropy and non-linearity in their biomechanical behaviour. In continuum-based models, this contribution is considered by incorporation of specialised strain energy functions that are associated with invariants I_4 and I_6, often either through '*Holzapfel- type*' functions (e.g. see [1] and [2] amongst others), their counterparts which accommodate fibre dispersion (e.g. [3-6]), or *Fung-type* models (e.g. [7,8]), to name but a few. The representation of the contribution of the '*isotropic matrix*', however, has remained rather elusive and considerably less specialised, often accounted for by a general neo-Hookean or an exponential term, as a function of the invariant I_1. Such generic phenomenological descriptions and mathematical representations, while may provide a good fit to the experimental data, do not shed much light on the specific mechanics of the contribution of the matrix (micro)structure to the observed tissue-level behaviour, and may therefore be less amenable to rigorous interpretation and analysis. Ideally, similar to the anisotropic part, specialised mathematical functions that are based on the physical/structural characteristics of the matrix are sought for incorporation into continuum-based models.

In the case of the aortic valve (AV) tissue, which is the subject of this paper, the non-collagenous matrix is mainly comprised of glycosaminoglycans (GAGs) and the elastin network. GAGs are not considered to contribute to the load-bearing capacity of the AV tissue, and are instead better known for their viscous-like rate-dependent properties. The interested reader may wish to refer to our recent study for a new continuum-based viscoelastic model [2] or our preceding studies for rheological modelling [9,10] of the rate-dependent anisotropic behaviour of the AV. Therefore, and by excluding the contribution of the GAGs, deformation of the '*isotropic matrix*'

in the AV shall mainly be characterised by the deformation of the elastin network. The pioneering work of Vesely (1998) established that the mechanical behaviour of the AV elastin network may be isotropic, by carrying out tensile deformation tests on intact network samples, further corroborating the notion that the mechanical behaviour of the '*isotropic matrix*' within the AV tissue mainly stems from the isotropic elastin network [11]. As such, the mathematical terms representing the '*isotropic matrix*' in continuum-based models developed to date for application to the AV are inadvertently associated with the behaviour of the elastin network. Those mathematical terms have almost exclusively been chosen to be represented by generic functions such as either a neo-Hookean term (e.g. [3]) or an exponential term (e.g. [2, 12-14]). A specialised function that is based on the biomechanical and structural characteristics of the AV elastin network has somehow been overlooked within the framework of continuum mechanics modelling of the AV tissue and is currently lacking in the literature.

The purpose of this paper is therefore to propose a customised energy function for the deformation of the AV elastin network that, while provides a good fit to the experimental data, is also structurally motivated. Following the well-established approach presented by Holzapfel et al. (2000) [1], we choose the following notations for terminologies pertaining to the elastic energy functions. The overall elastic energy function of the tissue W_e is considered to be the sum of the part that is associated with the isotropic deformation W_e^{iso} and the part that is associated with the anisotropic deformation W_e^{fibres}, i.e. $W_e = W_e^{iso} + W_e^{fibres}$. However, as explained above, the isotropic part is essentially the contribution of the elastin network. Therefore, the elastic energy function W_e of the AV tissue is considered as an additive split of the form:

$$W_e = W_e^{elastinnetwork} + W_e^{fibres} \tag{1}$$

Our aim is therefore to establish and propose a suitable $W_e^{elastinnetwork}$ function. In doing so, we employ the following approach. We present a customised $W_e^{elastinnetwork}$ function developed based on the premise that the structural and biomechanical attributes of the elastin network closely resemble the networks of freely jointed

molecular chains [15-17], adopting a similar framework utilised by Arruda and Boyce (1993) [18]. We then derive the ensuing stress-stretch and force-stretch relationships and fit these equations to the experimental data points collated from the study by Vesely (1998), which reports the force-stretch curves of intact AV elastin network specimens under uniaxial tension [11]. We follow the same procedure with the neo-Hookean and the general exponential energy functions as the commonly proposed functions in the literature for modelling the AV '*isotropic matrix'*, as well as the *Arruda-Boyce* model as the gold standard of the freely jointed chain network models. We show that our proposed $W_e^{elastinnetwork}$ function provides an excellent fit to the experimental data, alongside the general exponential and the *Arruda-Boyce* models, while the neo-Hookean function fails to adequately capture the deformation behaviour of the AV elastin network. However, we discuss that the exponential function is purely a phenomenological description, with no structural meaning attached to the model and its parameters. We further present the fitting results of the *Arruda-Boyce* model and demonstrate that despite providing one of the best fits, the parameters estimated by the *Arruda-Boyce* model are not mathematically and structurally valid for the AV elastin network. It is subsequently concluded that our presented $W_e^{elastinnetwork}$ function is the preferred choice, being structurally-based, mathematically valid and providing a good fit to the data. We therefore propose this function for incorporation into the continuum-based models applied to the AV, to represent the contribution of the '*isotropic matrix*' part of the overall isochoric strain-energy function of the whole tissue.

2 $W_e^{elastinnetwork}$ energy functions

In this section we present the neo-Hookean, the general exponential and the *Arruda-Boyce* models, as the currently established and utilised models in the literature, and propose our own model based on a customisation of the classical energy function of the freely jointed chain networks utilised by Arruda and Boyce (1993) in their seminal paper [18]. In the following, however, for the sake of completeness and for the interested reader, we first give a brief theoretical overview of the framework, adapted for the elastin network.

Concisely, the classical elasticity framework of the freely jointed chains centres on the principles of the theory of statistical mechanics originally developed for rubber elasticity. The theory applies to flexible molecular chain network structures that are formed by occasional cross-links between the chains [15,18,19]. In their undeformed state, chains can have many arbitrary configurations of nearly equal entropy, typically represented by statistical distributions. Perturbing the chains away from their equilibrium conformations generates entropic forces that oppose these deformations, which forms the basis of their mechanical behaviour and stress-strain response [16,19]. It is postulated that the elastin network in soft tissues, in general, resembles a close functional and structural analogy to these networks [15-17].

Elastin in the AV is known to be present in the form of a (3D) network with inter-fibre connections to collagen fibres [11,20,21]. A schematic of the network structure for a representative volume element (RVE) of the AV matrix is shown in Figure 1. In the context of microstructural modelling of soft tissues, an RVE is an assumed volume of the continuum that is large enough to represent the typical characteristics of the microstructure, while still small compared to the characteristic length scale of the microstructure, i.e. the tissue thickness [22]. Without the loss of generality, and for simplicity in the analysis, the RVE is chosen to be a cube element such that the elastin chains form its spatial diagonals (Figure 1b).

Following Kuhl et al. (2005) [16] and Zhang et al. (2005) [17], we use the chain networks analogy to apply the principles of statistical mechanics of freely jointed molecular chains to the AV elastin network in this RVE. According to the chain network theory, the free energy of a network of n chains per unit volume is equal to the sum of the elastic free energy of the individual chains [25,26]. Thus, for an assumed RVE, the entire network may be replaced by a system of a single chain in the local Cartesian coordinate system that accounts for the total sum of the elastic energy of the individual chains [19]. Accordingly, for the RVE in Figure 1b, let us consider the single elastin chain along the diagonal of the cube with sides of initial length a_0 in the direction of the Cartesian coordinate system unit vectors $\mathbf{e_1}$, $\mathbf{e_2}$ and $\mathbf{e_3}$, as shown in Figure 1c. The two end points, *A* and *B*, are fixed points of inter-fibre connection and the chain can assume any arbitrary configuration without changing the end points.

In the statistical treatment of a single chain, the geometry of the chain is idealised as a composition of N segments of equal length l, also known as Kuhn segment length, as shown in Figure 1c. The contour length L of the chain is then $L = Nl$. Let r denote the end to end distance of the chain in the deformed configuration and r_0 the unstrained chain distance in the undeformed configuration. The chain stretch is therefore:

$$\lambda_c = \frac{r}{r_0} \tag{2}$$

Since the chain can assume any arbitrary configuration between the two end points *A* and *B*, a probability density function may be used to characterise the possible configurations. Let us introduce the probability density function $p(\lambda_c)$, which describes the probability that a chain of contour length L takes a configuration characterised by the end to end distance r. A statistical treatment for the $p(\lambda_c)$ function that is valid for application to large deformations, pertinent to those endured by the AV, may be provided by the Langevin model introduced by James and Guth (1943) of the form [25]:

$$p(\lambda_c) = p_0 \exp\left[-N\left(\frac{\lambda_c}{\sqrt{N}}\beta + \ln\frac{\beta}{\sinh\beta} \right) \right] \tag{3}$$

where $\beta = \ell^{-1}(\frac{\lambda_c}{\sqrt{N}})$, $\ell(\beta) = \coth\beta - \frac{1}{\beta}$ is the well-known Langevin function and p_0 is a normalisation constant.

The entropy of a chain whose configuration is described by the probability function in equation (3) is governed by the Boltzmann's equation as: $s = k \ln p(\lambda_c)$, where k is the Boltzmann constant. For a purely elastic response, the free energy ψ may be obtained as: $\psi = -Ts$, where T is the absolute temperature (e.g. see [27]). Combining these two relationships:

$$\psi = -kT \ln p(\lambda_c) \tag{4}$$

Inserting equation (3) into (4) gives the free energy function of a single chain as:

$$\psi = NkT\left(\frac{\lambda_c}{\sqrt{N}}\ell^{-1}\left(\frac{\lambda_c}{\sqrt{N}}\right)+\ln\frac{\ell^{-1}\left(\frac{\lambda_c}{\sqrt{N}}\right)}{\sinh\ell^{-1}\left(\frac{\lambda_c}{\sqrt{N}}\right)}\right)+\psi_0 \tag{5}$$

where ψ_0 is a constant so that the free energy of the chain ψ would be zero in the undeformed configuration.

We now recall that our system of a single chain in the considered RVE (Figure 1c) was such that it would account for the total sum of the elastic energy of the individual chains. Assuming that the network was originally comprised of *n* chains of equal Kuhn segment length l per unit volume and all the chains stretch uniformly, the free energy of the network may then be (e.g. see [28]):

$$\psi_{network} = \sum_{i=1}^{n}\psi^i = n\psi \tag{6}$$

However, to be able to define the macroscopic deformation energy of the network, i.e. the deformation of the network due to application of a load at tissue (macro) level, the key aspect is to link the deformation of the chain to the macroscopic deformation of the tissue continuum. In a broad classification, the macro-to-micro transition of the deformation assumes either an *affine* or a *non-affine* transformation [29]. The *affine* transformation assumes that the deformation of the chain can be computed from the tensorial transformation of the global strain tensor [22]. The *non-affine* deformation assumes an indirect transformation of stretch and in general may take a relationship of the form $\lambda_c = f\lambda$, where λ is the macro-level principal stretch and f is a stretch field that acts on the *affine* stretch in a multiplicative format [29]. The assumption of affine deformation of the chains may be an idealization [18,30] and in a previous study we showed that the strain transformation from tissue level to the micro-structure in AV specimens under tensile deformation may not be affine, especially at larger strains [31]. However, there is no conclusive overall consensus on this point in the literature. For example, a recent study has shown that the fibre kinematics in the Mitral valve leaflets may be affine [32], while another study has questioned the assumption of affine kinematics in planar fibrous connective tissues in general [33]. We shall therefore proceed under the assumption of an affine relationship between the macro (tissue level) stretch λ and the chain stretch λ_c , as is customary in the bulk

of the existing literature. For an example of an analysis surrounding a non-affine transformation, the interested reader is referred to [29].

For the considered single chain in the undeformed network shown in Figure 1c, the unstrained end to end distance of the chain, r_0, is $r_0 = a_0\sqrt{3}$. After deformation, the end-to-end chain vector is given by $\mathbf{r} = a_0(\lambda_1\mathbf{e_1} + \lambda_2\mathbf{e_2} + \lambda_3\mathbf{e_3})$, where λ_1, λ_2 and λ_3 are the principal (macro) stretches. Hence, the magnitude of $\mathbf{r}$ will be:

$$r = a_0\sqrt{\lambda_1^2 + \lambda_2^2 + \lambda_3^2} \tag{7}$$

Substituting the above equation into equation (2):

$$\lambda_c = \sqrt{\frac{I_1}{3}} \tag{8}$$

where I_1 is the first principal invariant of the right Cauchy-Green deformation tensor and is given by $I_1 = \lambda_1^2 + \lambda_2^2 + \lambda_3^2$. Equation (8) represents the relationship between the macro and micro stretches for our network system.

With equations (6) and (8) available, the energy function for the deformation of the elastin network $W_e^{elastinnetwork}$ in relation to the deformation at tissue level can be derived. Noting that [29]:

$$W_e^{elastin\ network} = \psi_{network}(\sqrt{\frac{I_1}{3}}) \tag{9}$$

and by inserting equations (5) and (6) into (9):

$$W_e^{elastin\ network} = nkTN\left(\sqrt{\frac{I_1}{3N}}\ell^{-1}(\sqrt{\frac{I_1}{3N}}) + \ln\frac{\ell^{-1}(\sqrt{\frac{I_1}{3N}})}{\sinh\ell^{-1}(\sqrt{\frac{I_1}{3N}})}\right) + \psi_0 \tag{10}$$

Equation (10) represents the energy function for the AV elastin network as a function of I_1. Note that ψ_0 is a constant so that $W_e^{elastinnetwork}$ would be zero in the undeformed state. This equation is similar to that of the strain energy function used

by Arruda and Boyce (1993) [18], equation (7) therein, for chains in their representative cubic element. A similar relationship is also demonstrated for a full network model by Beatty (2003) [28].

2.1 $W_e^{elastinnetwork}$ based on Arruda-Boyce model

The inverse Langevin function $\ell^{-1}()$ appearing in equation (10) may be approximated via different methods. Arruda and Boyce (1993) chose a series expansion approximation, which using the first five terms may be given as [18]:

$$\left(W_e^{elastin\ network}\right)_{Arruda-Boyce} = nkT\left(\frac{1}{2}(I_1-3)+\frac{1}{20N}(I_1^2-9)+\frac{11}{1050\,N^2}(I_1^3-27)+\frac{19}{7000N^3}(I_1^4-81)+\frac{519}{673750N^4}(I_1^5-243)\right) \quad (11)$$

2.2 A customised $W_e^{elastinnetwork}$

We now present our customisation of the energy function presented in equation (10). An interesting property of equation (10) is (see Appendix A):

$$\frac{\partial W_e^{elastin\ network}}{\partial \mathbf{C}} = \frac{1}{2\sqrt{3}}nkT\sqrt{N}\,\frac{1}{\sqrt{I_1}}\,\ell^{-1}\left(\sqrt{\frac{I_1}{3N}}\right)\mathbf{I} \quad (12)$$

which may alternatively be re-written as:

$$\frac{\partial W_e^{elastin\ network}}{\partial I_1} = \frac{1}{2\sqrt{3}}nkT\sqrt{N}\,\frac{1}{\sqrt{I_1}}\,\ell^{-1}\left(\sqrt{\frac{I_1}{3N}}\right) \quad (13)$$

For reasons that we will discuss in section 6, we use a Padè approximation for the inverse Langevin function in equation (13) as [34]:

$$\ell^{-1}\left(\sqrt{\frac{I_1}{3N}}\right) \approx \frac{\sqrt{\frac{I_1}{3N}}\left(3-\left(\frac{I_1}{3N}\right)\right)}{1-\left(\frac{I_1}{3N}\right)} \quad (14)$$

Substituting the above equation into (13), we propose the following strain energy function for the AV elastin network:

$$W_e^{elastin\ network} = \frac{1}{6} nkT \left[I_1 - 6N \ln(I_1 - 3N) \right] + w_0 \tag{15}$$

where the constant w_0 may be viewed as a similar parameter to ψ_0 in equation (10), i.e. w_0 is a constant so that $W_e^{elastinnetwork}$ would be zero in the undeformed state where $I_1 = 1$; therefore: $w_0 = -\frac{1}{6} nkT \left[3 - 6N \ln(3 - 3N) \right]$. Substituting this expression into equation (15) yields the final form of our proposed $W_e^{elastin\ network}$ as:

$$W_e^{elastin\ network} = nkTN \left[\frac{1}{6N} (I_1 - 3) - \ln\left(\frac{I_1 - 3N}{3 - 3N} \right) \right] \tag{16}$$

2.3 Neo-Hookean $W_e^{elastinnetwork}$

It has been customary to model the '*isotropic matrix*' of soft tissues with a Neo-Hookean strain energy function of the form (e.g. see [1,3-5]):

$$\left(W_e^{elastin\ network} \right)_{neo-Hookean} = \frac{1}{2} C (I_1 - 3) \tag{17}$$

where *C* is a stress-like positive material parameter.

2.4 General exponential-type $W_e^{elastinnetwork}$

Sometimes, particularly in the literature pertaining to modelling heart valves, the contribution of the '*isotropic matrix*' is alternatively considered via a generic exponential-type function, in the form of (e.g. see [2, 12-14]):

$$\left(W_e^{elastin\ network} \right)_{exponentid-type} = \frac{1}{2} \alpha \left(\exp\left[\beta (I_1 - 3) \right] - 1 \right) \tag{18}$$

where α and β are positive stress-like and dimensionless model parameters, respectively.

3 Deriving the stress-strain relationships

We shall now derive the associated stress-strain (stretch) relationships for the AV elastin network, based on the strain energy functions $W_e^{elastin\ network}$ formulated by equations (11), (16), (17) and (18). Assuming incompressibility, the second Piola-Kirchhoff stress tensor **S** for the network may be obtained by:

$$\mathbf{S} = 2\frac{\partial W_e^{elastin\ network}}{\partial \mathbf{C}} - p\mathbf{C}^{-1} \tag{19}$$

where **C** is the right Cauchy-Green tensor, and p is the arbitrary Lagrangian multiplier enforcing the constraint of incompressibility. **C** is related to the deformation gradient tensor **F** by $\mathbf{C} = \mathbf{F}^{\mathrm{T}} \cdot \mathbf{F}$. We note that in a pure homogenous deformation, the components of the deformation gradient matrix **F** have a diagonal form $\mathrm{diag}[\lambda_1, \lambda_2, \lambda_3]$ in relation to the principal stretches. It therefore follows:

$$\mathbf{F} = \begin{bmatrix} \lambda_1 & 0 & 0 \\ 0 & \lambda_2 & 0 \\ 0 & 0 & \lambda_3 \end{bmatrix} \quad , \quad \mathbf{C} = \begin{bmatrix} \lambda_1^2 & 0 & 0 \\ 0 & \lambda_2^2 & 0 \\ 0 & 0 & \lambda_3^2 \end{bmatrix} \quad , \quad \mathbf{C}^{-1} = \begin{bmatrix} \lambda_1^{-2} & 0 & 0 \\ 0 & \lambda_2^{-2} & 0 \\ 0 & 0 & \lambda_3^{-2} \end{bmatrix} \tag{20}$$

The Cauchy stress $\boldsymbol{\sigma}$, also known as the true stress, is obtained from **S** using $\boldsymbol{\sigma} = \mathbf{FSF}^{\mathbf{T}}$. The components of **S** and subsequently $\boldsymbol{\sigma}$ tensors have been derived and presented in Appendix B, giving the stress-stretch expressions for the AV elastin network in the general 3D case under pure homogenous tissue-level deformation, for each of the energy functions $W_e^{elastin\ network}$ described by equations (11), (16), (17) and (18).

However, one underlying assumption in characterising and modelling the biomechanical behaviour of the AV tissue is the consideration that the test specimens are thin sheet 'membranes'. That is, because the thickness of the AV tissue is much smaller than the other two in-plane dimensions of the valve (by two orders of magnitude), the AV is considered as a planar tissue (see for example [2]). Therefore, appropriate ensuing assumptions shall be applied to equations (B3) to (B6), Appendix B, to further tailor those relationships for AV application. One such assumption is that for a thin membrane, the through-thickness (principal) Cauchy stress can be

approximated zero $\sigma_{33}=0$, from which an expression for *p* may be established. Additionally, due to incompressibility, $\lambda_3=\frac{1}{\lambda_1\lambda_2}$. Therefore, equations (36) to (39) may be re-written accordingly. For the *Arruda-Boyce* model:

$$(\boldsymbol{\sigma})_{Arruda-Boyce}\rightarrow\begin{cases}\sigma_{11}=nkT\left(1+\frac{I_1}{5N}+\frac{33I_1^2}{525N^2}+\frac{76I_1^3}{3500N^3}+\frac{2595I_1^4}{336875N^4}\right)\left(\lambda_1^2-\frac{1}{\lambda_1^2\lambda_2^2}\right)\\ \sigma_{22}=nkT\left(1+\frac{I_1}{5N}+\frac{33I_1^2}{525N^2}+\frac{76I_1^3}{3500N^3}+\frac{2595I_1^4}{336875N^4}\right)\left(\lambda_2^2-\frac{1}{\lambda_1^2\lambda_2^2}\right)\\ \sigma_{33}=0\end{cases} \tag{21}$$

Similarly, for our proposed $W_e^{elastin\ network}$:

$$(\boldsymbol{\sigma})_{elastin\ network}\rightarrow\begin{cases}\sigma_{11}=\frac{1}{3}nkT\ \frac{9N-I_1}{3N-I_1}\left(\lambda_1^2-\frac{1}{\lambda_1^2\lambda_2^2}\right)\\ \sigma_{22}=\frac{1}{3}nkT\ \frac{9N-I_1}{3N-I_1}\left(\lambda_2^2-\frac{1}{\lambda_1^2\lambda_2^2}\right)\\ \sigma_{33}=0\end{cases} \tag{22}$$

For the neo-Hookean model:

$$(\boldsymbol{\sigma})_{neo-Hookean}\rightarrow\begin{cases}\sigma_{11}=C\left(\lambda_1^2-\frac{1}{\lambda_1^2\lambda_2^2}\right)\\ \sigma_{22}=C\left(\lambda_2^2-\frac{1}{\lambda_1^2\lambda_2^2}\right)\\ \sigma_{33}=0\end{cases} \tag{23}$$

And finally for the general exponential model:

$$(\boldsymbol{\sigma})_{exponentid-type} \rightarrow \begin{cases} \sigma_{11} = \alpha\beta\left(\exp\left[\beta(I_1 - 3)\right]\right)\left(\lambda_1^2 - \dfrac{1}{\lambda_1^2\lambda_2^2}\right) \\ \sigma_{22} = \alpha\beta\left(\exp\left[\beta(I_1 - 3)\right]\right)\left(\lambda_2^2 - \dfrac{1}{\lambda_1^2\lambda_2^2}\right) \\ \sigma_{33} = 0 \end{cases} \tag{24}$$

Equations (21) to (24) represent the expressions that are applicable to modelling the stress-stretch behaviour of the AV elastin network under in-plane deformation.

4 Application to experimental data

Experimental studies regarding the mechanical behaviour of the isolated elastin network in AV tissue are very rare in the literature, mainly owing to the difficulties associated with isolating the intact elastin network form the rest of the microstructural constituents of the AV [11,21]. However, in a rare study of its kind by Vesely (1998), the mechanical behaviour of the intact elastin network within the AV tissue has been characterised and reported under uniaxial loading, in the principal circumferential and radial loading directions [11]. These loading directions are defined in Figure 1d in relation to an AV cusp. We will use this data in order to check the suitability, and validate the application, of the considered energy functions in this study for modelling the deformation behaviour of the AV elastin network.

Prior to application to the experimental data, we shall apply further adjustments to equations (20) to (23), in order to make them applicable to uniaxial tests. Denoting the stretch in the uniaxial loading direction and the transverse direction by λ_1 and λ_2, respectively, we note that $\lambda_2 = \lambda_3$ (where λ_3 is the stretch in the orthogonal

direction) with incompressibility dictating $\lambda_1 \cdot \lambda_2 \cdot \lambda_3 = 1$, therefore $\lambda_2^2 = \frac{1}{\lambda_1}$. Hence, equations (21) to (24) for uniaxial tensile deformations may take the following forms:

$$\begin{cases} (\sigma_{11})_{Arruda-Boyce} = nkT \left(1 + \frac{(\lambda_1^2 + 2\lambda_1^{-1})}{5N} + \frac{33(\lambda_1^2 + 2\lambda_1^{-1})^2}{525\,N^2} + \frac{76(\lambda_1^2 + 2\lambda_1^{-1})^3}{3500N^3} + \frac{2595(\lambda_1^2 + 2\lambda_1^{-1})^4}{336875N^4}\right)\left(\lambda_1^2 - \frac{1}{\lambda_1}\right) \\ (\sigma_{11})_{elastin\ network} = \frac{1}{3} nkT \ \frac{9N - (\lambda_1^2 + 2\lambda_1^{-1})}{3N - (\lambda_1^2 + 2\lambda_1^{-1})}\left(\lambda_1^2 - \frac{1}{\lambda_1}\right) \\ (\sigma_{11})_{neo-Hookean} = C\left(\lambda_1^2 - \frac{1}{\lambda_1}\right) \\ (\sigma_{11})_{exponentid-type} = \alpha\beta\left\{\exp\left[\beta\left((\lambda_1^2 + 2\lambda_1^{-1}) - 3\right)\right]\right\}\left(\lambda_1^2 - \frac{1}{\lambda_1}\right) \end{cases} \tag{25}$$

Note that σ_{11} and λ_1 represent the stress and the stretch along the loading direction, either the circumferential or the radial.

The data reported in Vesely (1998) is presented in the form of surface tension (N/m) versus stretch. Surface tension is the axial load per unit width of the specimen over which it is applied [11]. This force, denoted by **P** henceforth, may be determined from the second Piola-Kirchhoff stress tensor **S** by [35]:

$$\mathbf{P} = h\,\mathbf{F}\,\mathbf{S} \tag{26}$$

where *h* is the initial thickness of the specimen. Given the relationship between the second Piola-Kirchhoff stress **S** and the Cauchy stress $\boldsymbol{\sigma}$, the above equation can be rewritten as:

$$\mathbf{P} = h\,\boldsymbol{\sigma}\,(\mathbf{F}^{\mathrm{T}})^{-1} \tag{27}$$

Substituting for (σ_{11})s from equation (25) into (27), we determine the tension force as:

$$\begin{cases} (P_{11})_{Arruda-Boyce} = nhkT\left(1+\dfrac{(\lambda_1^2+2\lambda_1^{-1})}{5N}+\dfrac{33(\lambda_1^2+2\lambda_1^{-1})^2}{525\,N^2}+\dfrac{76(\lambda_1^2+2\lambda_1^{-1})^3}{3500N^3}+\dfrac{2595(\lambda_1^2+2\lambda_1^{-1})^4}{336875N^4}\right)\left(\lambda_1-\dfrac{1}{\lambda_1^2}\right) \\ (P_{11})_{elastin\ network} = \dfrac{1}{3}nhkT\ \dfrac{9N-(\lambda_1^2+2\lambda_1^{-1})}{3N-(\lambda_1^2+2\lambda_1^{-1})}\left(\lambda_1-\dfrac{1}{\lambda_1^2}\right) \\ (P_{11})_{neo-Hookean} = Ch\left(\lambda_1-\dfrac{1}{\lambda_1^2}\right) \\ (P_{11})_{exponentid-type} = \alpha\beta h\left\{\exp\left[\beta\left((\lambda_1^2+2\lambda_1^{-1})-3\right)\right]\right\}\left(\lambda_1-\dfrac{1}{\lambda_1^2}\right) \end{cases} \tag{28}$$

The expressions in equation (28) may now be applied to the experimental surface tension force-stretch data provided in Vesely (1998) [11]. Prior to this application, however, the convexity of our proposed $W_e^{elastin\ network}$ function given by equation (16) must be ensured. The analysis surrounding the strict local convexity of $W_e^{elastinnetwork}$ is presented in Appendix C. We shall also illustrate the projections of the contours of constant $W_e^{elastinnetwork}$ in (λ_1,λ_2) and (E_{11},E_{22}) planes in the following section, which reflect the convexity of $W_e^{elastinnetwork}$ graphically.

5 Results

The experimental surface tension force versus stretch data of the intact AV elastin network were collated from the graphs reported in Vesely (1998) [11]. The average failure strain and tension were reported to be approximately 135% (corresponding to $\lambda = 2.35$) and 2.2 Nm^{-1}, respectively. We used these values to select the representative curves which accommodated these characteristics, from which the data points were extracted. From the reported 8 specimens loaded radially, 6 curves fulfilled these attributes, while 11 out of the reported 15 specimens loaded in the circumferential direction showed these features. The relationships in equation (28) were then fitted to the collated data points of these specimens, using the Levenberg-

Marquardt algorithm by the curve-fitting toolbox in MATLAB®. We note that since each AV sample was excised from a separate leaflet in the original study, variations in the network parameters between the circumferentially and radially loaded samples are to be expected.

We start by presenting the results of the fit of our proposed model to the data. These are shown in the graphs of Figure 2, for six representative samples in the circumferential and radial loading directions. The model provides an excellent fit, with R^2 values in excess of 0.98. Based on these fits, model constants, i.e. the network parameters n and N, were established and are summarised in Table 1. As defined in section 2, n is the number of chains per unit volume, while N designates the Kuhn segment length (number of segments of equal length l in a chain). These parameters are inherent characteristics of the elastin network and are therefore the structural properties of the tissue and do not depend on the loading direction. The modelling outcomes also reflect this notion, as the calculated mean values for n and N are closely matched in both loading directions (Table 1). The characterisation of these parameters for the elastin network in AV tissue is currently lacking in the literature, to the knowledge of the authors, for a direct comparison of our results with other studies. However, the reported parameters in this study may be deemed comparable to the values reported in the literature for other soft tissues such as the arteries [17,36].

The plots for our proposed $W_e^{elastinnetwork}$ function in equation (16) and its contours in (λ_1, λ_2) and (E_{11}, E_{22}) planes, constructed using the average values of n and N (Table 1) are shown in Figure 3. Note that E_{11} and E_{22} represent the principal Green-Lagrange strains. The iso-energy contours graphically confirm the convexity of the proposed elastic energy function $W_e^{elastinnetwork}$.

We now present the fitting results of the other considered functions. The graphs in Figure 4 illustrate how the neo-Hookean model in equation $(28)_3$ fits to the data, for a representative sample in the circumferential and radial directions. As it can readily be observed, the neo-Hookean function fails to provide an acceptable fit. This lack of ability to describe the deformation behaviour of the AV elastin network by the neo-

Hookean function was repeatedly seen in all the other samples too, and we therefore refrain to illustrate the other ten curves here.

The graphs in Figure 5 represent the fitting results for the *Arruda-Boyce* model, as given in equation $(28)_1$. It may be observed that the *Arruda-Boyce* model too provides an excellent fit, with R^2 values in excess of 0.98. The average values of n and N calculated by this model were $n = 1.38 \times 10^{23}$ and $N = 2.39$ for the circumferentially loaded samples, and $n = 1.05 \times 10^{23}$ and $N = 2.16$ for the radial samples. We shall discuss these results, in particular the parameter N, in more depth in the next section.

The general exponential model also appears to provide a very good fit to the data, as shown by the graphs in Figure 6, with R^2 values similar to our proposed model and the *Arruda-Boyce* model.

In summary, judging by the quality of the fit to the data, the neo-Hookean model appears to be the least suitable choice for describing the deformation behaviour of the '*isotropic matrix*' in the AV tissue, represented by the AV elastin network. Our proposed model provides a very good fit; yet, the *Arruda-Boyce* and the general exponential models appear to provide even better results. However, a generic exponential function as given in equation (18) for strain energy may be less amenable to rigorous analysis and interpretation, as it is essentially a phenomenological model with no meaningful structurally-based material/model parameters. Therefore, such a model does not facilitate further insight into the mechanics of the contribution of the structure to the observed deformation behaviour of a tissue. This shortcoming may be considered a major disadvantage of such models. In this context, the more appropriate choices appear to be the *Arruda-Boyce* and our proposed models. In the following section we discuss the advantages and disadvantages of the two models, analysing the validity of the modelling outcomes, and conclude that our model is the preferred option.

6 Discussion

A customised model, based on the classical energy function of the freely jointed chain networks, was presented in this paper to model the behaviour of the AV elastin network under tensile deformation. We note that, while the employed principles are similar to those of Arruda and Boyce (1993) [18], the final form of the presented model is different to the *Arruda-Boyce* model, or indeed to its other branches including, for example, the one employed by Zou and Zhang (2009) [36]. This difference is mainly due to the consideration of isotropy, and more importantly the method chosen to approximate the inverse Langevin function.

The strain energy function employed in the *Arruda-Boyce* model is developed based on the (first five-term) series expansion of the inverse Langevin function, while our proposed model exploits the Padè approximation introduced by Cohen (1991) [34]. Comparing the two approximations, as illustrated in Figure 7a, it may be observed that the Padè approximation is indeed a more accurate representation of the inverse Langevin function within its entire domain, compared to the first five-term series expansion approximation. Therefore, while the *Arruda-Boyce* model provides a better fit, it is arguably a less accurate function in representing the whole-range behaviour of the inverse Langevin function. In particular, the inaccuracy of the series expansion approximation becomes more pronounced within the deformation domain, compared to the Padè approximation, as shown in the inset of Figure 7a, and for the corresponding ranges of I_1 as shown in Figure 7b, calculated using the average values of N given in Table 1.

In addition, inherent to the characteristics of the inverse Langevin function is its asymptotic behaviour, leading to singularity points. The series expansion approximation essentially eliminates this feature, while the employed Padè approximation preserves this inherent characteristic. The reason this point of discontinuity may be useful is that it would allow prediction of a limiting stretch, where the denominator $3N - I_1$ becomes zero, beyond which the network may not stretch. This characteristic would be an additional structural feature pertaining to the AV elastin network which will be accounted for by using our proposed model, while

it would be lost in an *Arruda-Boyce* model. As a representative example, using the average calculated values of *N* listed in Table 1 and $3N - I_1 = 0$, a limiting stretch in the range of $\lambda_1 = 3.02$ to $\lambda_1 = 3.16$ may be calculated by our model for the elastin network in the tested AV samples. Noting the reported force-stretch data in Figure 2, the maximum reported stretch of the network falls well within this upper limit. The estimated limiting stretch by our model may be viewed as the theoretical upper limit of the stretch of an ideal network. Samples used in experiments would therefore inevitably show lower failure values due to experimental artefacts such as the structural damages inflicted by the use of digestion assays, the gripping effects etc. .

However, and more importantly than the above two points, or perhaps as a result of the above two points, the values for *N* calculated by the *Arruda-Boyce* model are not mathematically or structurally valid for the AV elastin network. Recalling from section 5, the *Arruda-Boyce* model calculates average *N* values of *N* = 2.39 and *N* = 2.16 for the circumferentially and radially loaded samples, respectively. However, the inverse Langevin function $\ell^{-1}(x)$ is only defined in the domain $-1 < x < 1$. In view of equation (10) for $\ell^{-1}(\sqrt{\frac{I_1}{3N}})$, it follows that $-1 < \sqrt{\frac{I_1}{3N}} < 1$, which requires *a priori* $N > \frac{I_1}{3}$. As may be observed in Figure 5, the average maximum stretch of the elastin network λ_1 in the circumferential direction is $\lambda_1 = 2.68$, and in radial direction is $\lambda_1 = 2.64$, resulting in I_1 values of $I_1 = 7.93$ and $I_1 = 7.71$ in the respective directions. Therefore, the calculated *N* values by the *Arruda-Boyce* model do not satisfy the *a priori* requirement of $N > \frac{I_1}{3}$, and are subsequently mathematically invalid. The structural interpretation of not satisfying the above requirement is that, if the Kuhn segments *N* of the elastin network were indeed those of the *Arruda-Boyce* model, the network had stretched beyond the point where all chains were fully straight, which is not theoretically admissible. No such issue arises by the application of our proposed $W_e^{elastinnetwork}$ function (see Table 1 and Figure 2).

The advantages of the application of our model come of course at a cost: potentially due to the preservation of the original inverse Langevin function's asymptotic

characteristic in our model, the convergence in the fittings may be less easily achievable. However, this risk can be mitigated by employing simple numerical approaches that can estimate a reasonably narrow range within which the global minima may exist, and use those ranges as the guide for initiation of the fitting process in MATLAB® using the curve-fitting toolbox. This approach was used in this study and other robust and more optimal approaches may also be devised and applied. Therefore, on balance, our proposed model appears to provide a good fit to the data, the modelling results are mathematically and structurally valid, and the fitting pre-requisites are relatively straight forward.

We note that the general exponential model also provided a good fit to the experimental data (Figure 6). However, the exponential model is essentially a phenomenological model and the parameters α and β do not have any structural meaning attached to them. Therefore, if one's goal is to model the deformation behaviour of the whole tissue based on its structural characteristics, the application of such phenomenological models will not be useful. The other phenomenological model considered in this study, i.e. the neo-Hookean model, is not suitable for fitting to the AV elastin network deformation data either, as indicated by the results (Figure 4). We therefore do not recommend the application of either of these two strain energy functions to structurally-motivated continuum-based modelling of the AV tissue.

As an alternative approach for quantifying the structural parameters n and N, we fitted all the twelve experimental datasets used in this study simultaneously to our model given in equation $(28)_2$ by a custom-developed code in MATLAB®, minimising the residual sum of squares (RSS) function defined as: $\mathrm{RSS} = \sum_i \left(P_{11}^{Model} - P_{11}^{Experiment} \right)_i^2$. P_{11}^{Model} in this function is the tension calculated by the model, $P_{11}^{Experiment}$ is the experimental tension and i is the number of datasets. The calculated values using this approach are $n = 1.67 \times 10^{23}$ and $N = 3.36$, resulting from fits with a maximum RSS = 2.711 and R^2 values in excess of 0.973. These values are very close to those summarised in Table 1, and further reinforce the isotropy of the elastin network and the independence of the values of n and N from the loading direction.

One of the important outcomes of this study is the underpinning of a specialised strain energy function associated with the contribution of the elastin network $W_e^{elastinnetwork}$. This strain energy function facilitates a step forward in developing fully structurally motivated continuum-based models to analyse and simulate the biomechanical behaviour of the AV. For studies wishing to employ strain energy functions in the form presented in equation (1), the devised $W_e^{elastinnetwork}$ in this paper (equation (16)) can be superimposed onto the existing strain energy functions associated to the collagen fibres' family W_e^{fibres}, e.g. '*Holzapfel type*' strain energy functions, to account for contributions of the isotropic matrix as well as the anisotropic collagen fibre family. While, due to the limited availability of the experimental data on the deformation of the intact elastin network in the AV, the model was applied to uniaxial tensile data, the general 3D and 2D formulations were derived and presented here. The uniaxial application of the model was tailored through the incorporation of the appropriate mechanistic and mathematical assumptions detailed in sections 3, 4 and Appendix B, and does not reflect any inhibitions on the general applicability of the devised model and the strain energy function.

Appendix A: Calculating $\dfrac{\partial W_e^{elastin\ network}}{\partial \mathbf{C}}$

Invoking the chain rule, we note that: $\dfrac{\partial W_e^{elastin\ network}}{\partial \mathbf{C}} = \dfrac{\partial W_e^{elastin\ network}}{\partial I_1} \cdot \dfrac{\partial I_1}{\partial \mathbf{C}}$, where $W_e^{elastinnetwork}$ is defined by equation (10). Therefore:

$$\frac{\partial W_e^{elastin\ network}}{\partial I_1} = nkTN\ \ell^{-1}\left(\sqrt{\frac{I_1}{3N}}\right)\frac{\partial}{\partial I_1}\sqrt{\frac{I_1}{3N}} + nkTN\sqrt{\frac{I_1}{3N}}\ \frac{\partial}{\partial I_1}\ell^{-1}\left(\sqrt{\frac{I_1}{3N}}\right)$$

$$+ nkTN\frac{\partial}{\partial I_1}\ln\frac{\ell^{-1}\left(\sqrt{\frac{I_1}{3N}}\right)}{\sinh\ell^{-1}\left(\sqrt{\frac{I_1}{3N}}\right)} \qquad \text{(A1)}$$

Using the change of variable $\ell^{-1}\left(\sqrt{\frac{I_1}{3N}}\right) = X$, the above equation simplifies to:

$$\frac{\partial W_e^{elastin\ network}}{\partial I_1} = nkTN\ X\frac{\partial}{\partial I_1}\sqrt{\frac{I_1}{3N}} + nkTN\sqrt{\frac{I_1}{3N}}\ \frac{\partial X}{\partial I_1} + nkTN\frac{\partial}{\partial I_1}\ln\frac{X}{\sinh X} \qquad \text{(A2)}$$

However, in the above equation we note that:

$$\frac{\partial}{\partial I_1}\ln\frac{X}{\sinh X} = \frac{\partial\ln\frac{X}{\sinh X}}{\partial X}\cdot\frac{\partial X}{\partial I_1} = \frac{\sinh(X) - X\cosh(X)}{X\sinh(X)}\cdot\frac{\partial X}{\partial I_1} = \left(\frac{1}{X} - \coth(X)\right)\cdot\frac{\partial X}{\partial I_1} \qquad \text{(A3)}$$

where $\dfrac{1}{X} - \coth(X) = -\ell(X) = -\ell\left(\ell^{-1}\left(\sqrt{\frac{I_1}{3N}}\right)\right) = -\sqrt{\frac{I_1}{3N}}$. Therefore, equation (A2) becomes:

$$\frac{\partial W_e^{elastin\ network}}{\partial I_1} = nkTN\ X\frac{\partial}{\partial I_1}\sqrt{\frac{I_1}{3N}} + nkTN\sqrt{\frac{I_1}{3N}}\ \frac{\partial X}{\partial I_1} - nkTN\sqrt{\frac{I_1}{3N}}\frac{\partial X}{\partial I_1} = nkTN\ X\frac{\partial}{\partial I_1}\sqrt{\frac{I_1}{3N}} \qquad \text{(A4)}$$

Noting that $\frac{\partial I_1}{\partial \mathbf{C}} = \frac{\partial \mathrm{tr}\mathbf{C}}{\partial \mathbf{C}} = \mathbf{I}$, $\frac{\partial W_e^{elastin\ network}}{\partial \mathbf{C}}$ can be determined as:

$$\frac{\partial W_e^{elastin\ network}}{\partial \mathbf{C}} = nkTN\,\ell^{-1}\left(\sqrt{\frac{I_1}{3N}}\right)\frac{\partial}{\partial I_1}\sqrt{\frac{I_1}{3N}}\;\mathbf{I} = \frac{1}{2\sqrt{3}}nkT\sqrt{N}\,\frac{1}{\sqrt{I_1}}\,\ell^{-1}\left(\sqrt{\frac{I_1}{3N}}\right)\mathbf{I} \qquad \text{(A5)}$$

Appendix B: Deriving the second Piola-Kirchhoff stress S and the Cauchy stress $\boldsymbol{\sigma}$ tensors

Using the chain rule, $\dfrac{\partial W_e^{\,elastin\ network}}{\partial \mathbf{C}}$ for the strain energy functions given by equations (11), (16), (17) and (18) may be obtained as:

$$\begin{cases} \dfrac{\partial \left(W_e^{\,elastin\ network}\right)_{Arruda-Boyce}}{\partial \mathbf{C}} = nkT\left(\dfrac{1}{2}+\dfrac{I_1}{10N}+\dfrac{33I_1^2}{1050\,N^2}+\dfrac{76I_1^3}{7000N^3}+\dfrac{2595I_1^4}{673750N^4}\right)\mathbf{I} \\ \dfrac{\partial W_e^{\,elastin\ network}}{\partial \mathbf{C}} = \dfrac{1}{6}nkT\ \dfrac{9N-I_1}{3N-I_1}\ \mathbf{I} \\ \dfrac{\partial \left(W_e^{\,elastin\ network}\right)_{neo-Hookean}}{\partial \mathbf{C}} = \dfrac{1}{2}\ C\ \mathbf{I} \\ \dfrac{\partial \left(W_e^{\,elastin\ network}\right)_{exponentid-type}}{\partial \mathbf{C}} = \dfrac{1}{2}\ \alpha\beta\exp\left[\beta(I_1-3)\right]\mathbf{I} \end{cases} \tag{B1}$$

In view of equation (19), the ensuing Piola-Kirchhoff stress **S** tensors pertaining to each $W_e^{\,elastin\ network}$ for pure homogenous deformations are achieved as:

$$
\begin{cases}
(\mathbf{S})_{Arruda-Boyce} = nkT\left(1+\dfrac{I_1}{5N}+\dfrac{33I_1^2}{525N^2}+\dfrac{76I_1^3}{3500N^3}+\dfrac{2595I_1^4}{336875N^4}\right)\begin{bmatrix}1&0&0\\0&1&0\\0&0&1\end{bmatrix}-p\begin{bmatrix}\lambda_1^{-2}&0&0\\0&\lambda_2^{-2}&0\\0&0&\lambda_3^{-2}\end{bmatrix} \\
(\mathbf{S})_{elastin\ network} = \dfrac{1}{3}nkT\ \dfrac{9N-I_1}{3N-I_1}\begin{bmatrix}1&0&0\\0&1&0\\0&0&1\end{bmatrix}-p\begin{bmatrix}\lambda_1^{-2}&0&0\\0&\lambda_2^{-2}&0\\0&0&\lambda_3^{-2}\end{bmatrix} \\
(\mathbf{S})_{neo-Hookean} = C\begin{bmatrix}1&0&0\\0&1&0\\0&0&1\end{bmatrix}-p\begin{bmatrix}\lambda_1^{-2}&0&0\\0&\lambda_2^{-2}&0\\0&0&\lambda_3^{-2}\end{bmatrix} \\
(\mathbf{S})_{exponentid-type} = \alpha\beta\exp\left[\beta(I_1-3)\right]\begin{bmatrix}1&0&0\\0&1&0\\0&0&1\end{bmatrix}-p\begin{bmatrix}\lambda_1^{-2}&0&0\\0&\lambda_2^{-2}&0\\0&0&\lambda_3^{-2}\end{bmatrix}
\end{cases}
\tag{B2}
$$

Using $\boldsymbol{\sigma} = \mathbf{FSF}^{\mathbf{T}}$, the components of the Cauchy stress (i.e. the true stress) may be obtained as follows. For the Arruda-Boyce model:

$$
(\boldsymbol{\sigma})_{Arruda-Boyce} \rightarrow \begin{cases}
\sigma_{11} = nkT\left(1+\dfrac{I_1}{5N}+\dfrac{33I_1^2}{525N^2}+\dfrac{76I_1^3}{3500N^3}+\dfrac{2595I_1^4}{336875N^4}\right)\lambda_1^2-p \\
\sigma_{22} = nkT\left(1+\dfrac{I_1}{5N}+\dfrac{33I_1^2}{525N^2}+\dfrac{76I_1^3}{3500N^3}+\dfrac{2595I_1^4}{336875N^4}\right)\lambda_2^2-p \\
\sigma_{33} = nkT\left(1+\dfrac{I_1}{5N}+\dfrac{33I_1^2}{525N^2}+\dfrac{76I_1^3}{3500N^3}+\dfrac{2595I_1^4}{336875N^4}\right)\lambda_3^2-p
\end{cases}
\tag{B3}
$$

For our proposed $W_e^{elastin\ network}$:

$$(\boldsymbol{\sigma})_{elastin\ network} \rightarrow \begin{cases} \sigma_{11} = \frac{1}{3} nkT \ \frac{9N - I_1}{3N - I_1} \lambda_1^2 - p \\ \sigma_{22} = \frac{1}{3} nkT \ \frac{9N - I_1}{3N - I_1} \lambda_2^2 - p \\ \sigma_{33} = \frac{1}{3} nkT \ \frac{9N - I_1}{3N - I_1} \lambda_3^2 - p \end{cases} \tag{B4}$$

For the neo-Hookean model:

$$(\boldsymbol{\sigma})_{neo-Hookean} \rightarrow \begin{cases} \sigma_{11} = C\,\lambda_1^2 - p \\ \sigma_{22} = C\,\lambda_2^2 - p \\ \sigma_{33} = C\,\lambda_3^2 - p \end{cases} \tag{B5}$$

And finally for the general exponential model:

$$(\boldsymbol{\sigma})_{exponentid-type} \rightarrow \begin{cases} \sigma_{11} = \alpha\beta \exp\left[\beta(I_1 - 3)\right] \lambda_1^2 - p \\ \sigma_{22} = \beta \exp\left[\beta(I_1 - 3)\right] \lambda_2^2 - p \\ \sigma_{33} = \beta \exp\left[\beta(I_1 - 3)\right] \lambda_3^2 - p \end{cases} \tag{B6}$$

Appendix C: Convexity of the proposed $W_e^{elastin\ network}$

The condition of 'strict local convexity' for $W_e^{elastinnetwork}$ requires that the Hessian of $W_e^{elastinnetwork}$ to be positive definite. The Hessian matrix, in relation to λ is defined as:

$$\mathbf{H} = \begin{bmatrix} \dfrac{\partial^2 W_e^{elastin\ network}}{\partial \lambda_1^2} & \dfrac{\partial^2 W_e^{elastin\ network}}{\partial \lambda_1 \partial \lambda_2} \\ \dfrac{\partial^2 W_e^{elastin\ network}}{\partial \lambda_2 \partial \lambda_1} & \dfrac{\partial^2 W_e^{elastin\ network}}{\partial \lambda_2^2} \end{bmatrix} \tag{C1}$$

where **H** denotes the Hessian matrix. Calculating the terms $\dfrac{\partial^2 W_e^{elastin\ network}}{\partial \lambda_1 \partial \lambda_2}$ and $\dfrac{\partial^2 W_e^{elastin\ network}}{\partial \lambda_2 \partial \lambda_1}$ in view of equation (16), it may be observed that $\dfrac{\partial^2 W_e^{elastin\ network}}{\partial \lambda_1 \partial \lambda_2} = \dfrac{\partial^2 W_e^{elastin\ network}}{\partial \lambda_2 \partial \lambda_1} = 4nkTN \cdot \dfrac{\lambda_1 \lambda_2}{(3N - I_1)^2}$, and hence **H** is symmetrical. Therefore, in order for **H** to be positive definite, it is necessary that $\dfrac{\partial^2 W_e^{elastin\ network}}{\partial \lambda_1^2}$, $\dfrac{\partial^2 W_e^{elastin\ network}}{\partial \lambda_2^2}$, det (**H**) and the eigenvalues of **H** are all positive. Thus:

$$\begin{cases} \dfrac{\partial^2 W_e^{elastin\ network}}{\partial \lambda_1^2} > 0 \Rightarrow \dfrac{12\lambda_1^2 N}{(3N - I_1)^2} > -\dfrac{9N - I_1}{3N - I_1} \\ \dfrac{\partial^2 W_e^{elastin\ network}}{\partial \lambda_2^2} > 0 \Rightarrow \dfrac{12\lambda_2^2 N}{(3N - I_1)^2} > -\dfrac{9N - I_1}{3N - I_1} \\ \det(\mathbf{H}) > 0 \Rightarrow \left(\dfrac{9N - I_1}{3N - I_1}\right)^2 > -\dfrac{12N(9N - I_1)(\lambda_1^2 + \lambda_2^2)}{(3N - I_1)^3} \\ eigenvalues(\mathbf{H}) > 0 \Rightarrow \text{both roots of the 'characteristic equation' must be positive} \end{cases} \tag{C2}$$

It may readily be observed that all the above four inequalities are satisfied *a priori* for $N > \frac{I_1}{3}$ and $N < \frac{I_1}{3}$. Therefore, $W_e^{elastinnetwork}$ given in equation (16) satisfies the condition of strict local convexity. Note, however, that from a mathematical point of view, the inverse Langevin function $\ell^{-1}(x)$ is only defined within the domain of $-1 < x < 1$, which for the variable $\sqrt{\frac{I_1}{3N}}$ is equivalent to $-1 < \sqrt{\frac{I_1}{3N}} < 1$, requiring *a priori* $N > \frac{I_1}{3}$.

References

[1] Holzapfel, G.A., Gasser, T.C., and Ogden, R.W., 2000, "A new constitutive framework for arterial wall mechanics and a comparative study of material models", J. Elasticity, **61**, pp. 1-48.

[2] Anssari-Benam, A., Bucchi, A., Screen, H.R.C., and Evans, S.L., 2017, "A transverse isotropic viscoelastic constitutive model for the aortic valve tissue", R. Soc. Open Sci., **4**, 160585 (DOI: 10.1098/rsos.160585).

[3] Freed, A.D., Einstein, D.R., and Vesely, I., 2005, "Invariant formulation for dispersed transverse isotropy in aortic heart valves: an efficient means for modeling fiber splay", Biomech. Model. Mechanobiol., **4**, pp. 100-117.

[4] Gasser, T.C., Ogden, R.W., Holzapfel, G.A., 2006, "Hyperelastic modelling of arterial layers with distributed collagen fibre orientation", J. R. Soc. Interface, **3**, pp. 15-35.

[5] Holzapfel, G.A., and Ogden, R.W., 2010, "Constitutive modelling of arteries", Proc. R. Soc. A, **466**, pp. 1551-1597.

[6] Holzapfel, G.A., Niestrawska, J.A., Ogden, R.W., Reinisch, A.J., and Schriefl, A.J., 2015, "Modelling non-symmetric collagen fibre dispersion in arterial walls", J. R. Soc. Interface, **12**, 20150188 (DOI: 10.1098/rsif.2015.0188).

[7] Humphrey, J.D., 2003, "Review Paper: Continuum biomechanics of soft biological tissues", Proc. R. Soc. Lond. A, **459**, pp. 3-46.

[8] Holzapfel, G.A., 2006, "Determination of material models for arterial walls from uniaxial extension tests and histological structure", J. Theor. Biol., **238**, pp. 290-302.

[9] Anssari-Benam, A., Bader, D.L., and Screen, H.R.C., 2011, "A combined experimental and modelling approach to aortic valve viscoelasticity in tensile deformation", J. Mater. Sci. Mater. Med., **22**, pp. 253-262.

[10] Anssari-Benam, A., Barber, A.H., and Bucchi, A., 2016, "Evaluation of bioprosthetic heart valve failure using a matrix-fibril shear stress transfer approach", J. Mater. Sci. Mater. Med., **27**, 42 (DOI: 10.1007/s10856-015-5657-2).

[11] Vesely, I., 1998, "The role of elastin in aortic valve mechanics", J. Biomech., **31**, pp. 115-123.

[12] Weinberg, E.J., and Kaazempur-Mofrad, M.R., 2005, "On the constitutive models for heart valve leaflet mechanics", Cardiovasc. Eng., **5**, pp. 37-43.

[13] Weinberg, E.J., and Kaazempur Mofrad, M.R., 2007, "Transient, three-dimensional, multiscale simulations of the human aortic valve", Cardiovasc. Eng., **7**, pp. 140-155.

[14] Weinberg, E.J., Shahmirzadi, D., and Kaazempur Mofrad, M.R., 2010, "On the multiscale modeling of heart valve biomechanics in health and disease", Biomech. Model. Mechanobiol., **9**, pp. 373-387.

[15] Bischoff, J.E., Arruda, E.M., and Grosh, K., 2002, "Orthotropic hyperelasticity in terms of an arbitrary molecular chain model", J. Appl. Mech., **69**, pp. 198-201.

[16] Kuhl, E., Garikipati, K., Arruda, E.M., and Grosh, K., 2005, "Remodeling of biological tissue: mechanically induced reorientation of a transversely isotropic chain network", J. Mech. Phys. Solids, **53**, pp. 1552-1573.

[17] Zhang, Y., Dunn, M.L., Drexler, E.S., McCowan, C.N., Slifka, A.J., Ivy, D.D., and Shandas, R., 2005, "A microstructural hyperelastic model of pulmonary arteries under normo- and hypertensive conditions", Annals Bioemd. Eng., **33**, pp. 1042-1052.

[18] Arruda, E.M., and Boyce, M.C., 1993, "A three-dimensional constitutive model for the large stretch behavior of rubber elastic materials", J. Mech. Phys. Solids, **41**, pp. 389-412.

[19] Elias-Zuniga, A., and Beatty, M.F., 2002, "Constitutive equations for amended non-Gaussian network models of rubber elasticity", Int. J. Eng. Sci., **40**, pp. 2265-2294.

[20] Scott, M., and Vesely, I., 1995, "Aortic valve cusps microstructure: the role of elastin", Ann. Thorac. Surg., **60**, pp. S391-S394.

[21] Tseng, H., and Grande-Allen, K.J., 2011, "Elastic fibers in the aortic valve spongiosa: a fresh perspective on its structure and role in overall tissue function", Acta Biomater., **7**, pp. 2101-2108.

[22] Sacks, M.S., 2003, "Incorporation of experimentally-derived fiber orientation into a structural constitutive model for planar collagenous tissues". J. Biomech. Eng., **125**, pp. 280-287.

[23] Lewinsohn, A.D., Anssari-Benham, A., Lee, D.A., Taylor, P.M., Chester, A.H., Yacoub, M.H., and Screen, H.R.C., 2011, "Anisotropic strain transfer through the aortic valve and its relevance to the cellular mechanical environment", Proc. Inst. Mech. Eng. H, **225**, pp. 821-830.

[24] Rock, C.A., Han, L., and Doehring, T.C., 2014, "Complex collagen fiber and membrane morphologies of the whole porcine aortic valve", PLoS One, **9**, e86087 (DOI: 10.1371/journal.pone.0086087).

[25] James, H.M., and Guth, E., 1943, "Theory of the elastic properties of rubber", J. Chem. Phys., **11**, pp. 455-481.

[26] Treloar, L.R.G., 1954, "The photoelastic properties of short-chain molecular networks", Trans. Faraday Soc., **50**, pp. 881-896.

[27] Anssari-Benam, A., Viola, G., and Korakianitis, T., 2010, "Thermodynamic effects of linear dissipative small deformations", J. Therm. Anal. Calorim., **100**, pp. 941-947.

[28] Beatty, M.F., 2003, "An average-stretch full-network model for rubber elasticity", J. Elasticity, **70**, pp. 65-86.

[29] Miehe, C., Göktepe, S., and Lulei, F., 2004, "A micro-macro approach to rubber-like materials - Part I: the non-affine micro-sphere model of rubber elasticity", J. Mech. Phy. Solids, **52**, pp. 2617-2660.

[30] Boyce, M.C., and Arruda, E.M., 2000, “Constitutive models of rubber elasticity: a review”, Rubber Chem. Technol., **73**, pp. 504-523.

[31] Anssari-Benam, A., Gupta, H.S., and Screen, H.R.C., 2012, “Strain transfer through the aortic valve”, J. Biomech. Eng., **134**, 061003 (DOI: 10.1115/1.4006812).

[32] Lee, C.-H., Zhang, W., Liao, J., Carruthers, C.A., Sacks, J.I., Sacks, M.S., 2015, “On the presence of affine fibril and fiber kinematics in the Mitral valve anterior leaflet”, Biophys. J., **108**, 2074-2087.

[33] Jayyosi, C., Affagard, J.S., Ducourthial, G., Bonod-Bidaud, C., Lynch, B., Bancelin, S., Ruggiero, F., Schanne-Klein, M.C., Allain, J.M., Bruyère-Garnier, K., Coret, M., 2017, “Affine kinematics in planar fibrous connective tissues: an experimental investigation”, Biomech. Model Mechanobiol., DOI: 10.1007/s10237-017-0899-1.

[34] Cohen, A., 1991, “A Padé approximant to the inverse Langevin function”, Rheol. Acta, **30**, pp. 270-273.

[35] Billiar, K.L., and Sacks, M.S., 2000, “Biaxial mechanical properties of the natural and glutaraldehyde treated aortic valve cusp – part II: A structural constitutive model”, J. Biomech. Eng., **122**, pp. 327-335.

[36] Zou, Y., Zhang, Y., 2009, “An experimental and theoretical study on the anisotropy of elastin network”, Annals Bioemd. Eng., **37**, pp. 1572-1583.

Table legends

Table 1- Model parameters for intact AV elastin network samples loaded in the circumferential and radial directions.

Table 1

Constants			Model Parameters					
h (mm)	k (JK^{-1})	T (K)	Circumferential			Radial		
0.5*	1.38×10^{-23}	300	n (m^{-3})	N	R^2	n (m^{-3})	N	R^2
	Sample No.1		2.02×10^{23}	3.24	0.99	2.09×10^{23}	3.35	0.99
	Sample No.2		2.13×10^{23}	3.39	0.99	1.59×10^{23}	3.15	0.98
	Sample No.3		1.90×10^{23}	3.39	0.99	1.05×10^{23}	3.29	0.98
	Sample No.4		1.72×10^{23}	3.55	0.99	1.11×10^{23}	3.09	0.98
	Sample No.5		1.53×10^{23}	3.56	0.98	1.50×10^{23}	3.35	0.99
	Sample No.6		1.46×10^{23}	3.56	0.99	1.17×10^{23}	3.39	0.98
	Mean		1.79×10^{23}	3.45		1.42×10^{23}	3.27	

* As reported in [11].

Figure legends

Figure 1- (a) AV cut open: 3 leaflets of the valve attached to the aortic root (adopted from [23]); (b) Schematic of a leaflet's cross-section (adopted from [24]) and an idealised elastin network structure for a representative volume element (RVE) of an AV leaflet; (c) Geometry of a single elastin chain in a 3D cube RVE; and (d) The two principal loading directions of the AV leaflet: circumferential and radial.

Figure 2- Experimental and modelling tension-stretch data for the intact AV elastin network in: (a) the circumferential; and (b) the radial loading directions for 6 representative datasets. The experimental data points were collated from [11]. The markers represent the experimental data points and the continuous lines represent the modelling outcomes.

Figure 3- (a) The energy function $W_e^{elastinnetwork}$ proposed in equation (16) plotted versus λ_1 and λ_2; (b) the contours of $W_e^{elastinnetwork}$ in (λ_1, λ_2) plane; and (c) in (E_{11}, E_{22}) plane, for mean values of *n* and *N* (see Table 1). The graphs highlight the convexity of the proposed strain energy function.

Figure 4- A representative example of how the neo-Hookean model in equation $(28)_3$ provides a fit to the experimental data for: (a) circumferential sample; and (b) radial sample. The fitting results demonstrate the unsuitability of this function for characterising the behaviour of the AV elastin network, i.e. the AV '*isotropic matrix*'.

Figure 5- Experimental data fitted using the *Arruda-Boyce* model in equation $(28)_1$: (a) samples loaded in the circumferential direction; and (b) samples loaded in the radial direction. The markers represent the experimental data points and the continuous lines show the model predications.

Figure 6- Experimental data fitted using the general exponential model in equation $(28)_4$: (a) samples loaded in the circumferential direction; and (b) samples loaded in the radial direction. The markers represent the experimental data points, and the continuous lines show the model predications.

Figure 7- Comparison between the inverse Langevin function versus its series expansion (first five terms) and Padè approximations: (a) Padè approximation provides a more accurate description of the original function in the entire domain compared with the series expansion approximation. The typical deformation domain is shown in the inset; (b) Plots of the inverse Langevin, its series expansion and Padè approximation functions versus I_1 for the average values of *N* calculated in Table 1. Note that in all panels the hollow circles represent the inverse Langevin function, while the dotted and continuous lines represent the series expansion and the Padè approximations, respectively.

Figure 1

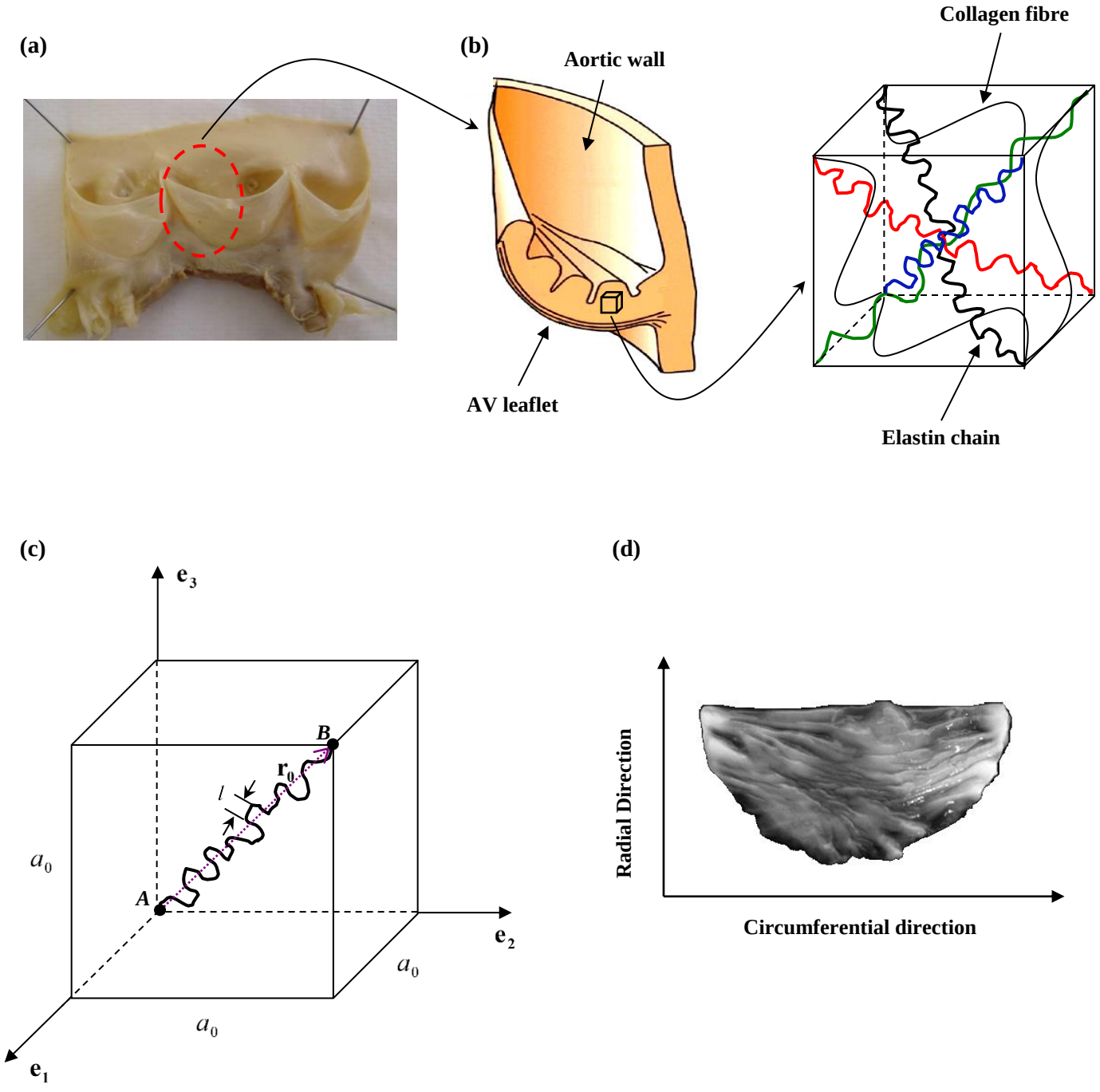
(a)
(b)
Aortic wall
Collagen fibre
AV leaflet
Elastin chain
(c)
$\mathbf{e}_3$
$\mathbf{e}_2$
$\mathbf{e}_1$
B
A
$\mathbf{r}_0$
l
a_0
a_0
a_0
(d)
Radial Direction
Circumferential direction

Figure 2

(a)

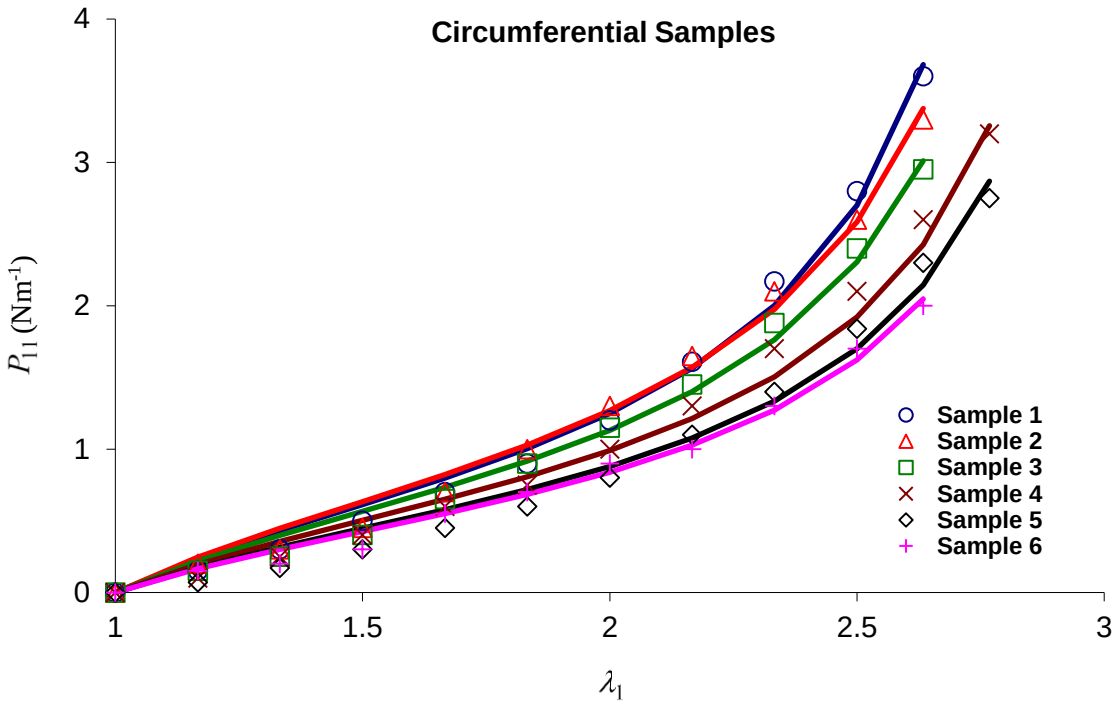
Circumferential Samples
P_{11} (Nm^{-1})
λ_1
0
1
2
3
4
1
1.5
2
2.5
3
Sample 1
Sample 2
Sample 3
Sample 4
Sample 5
Sample 6

(b)

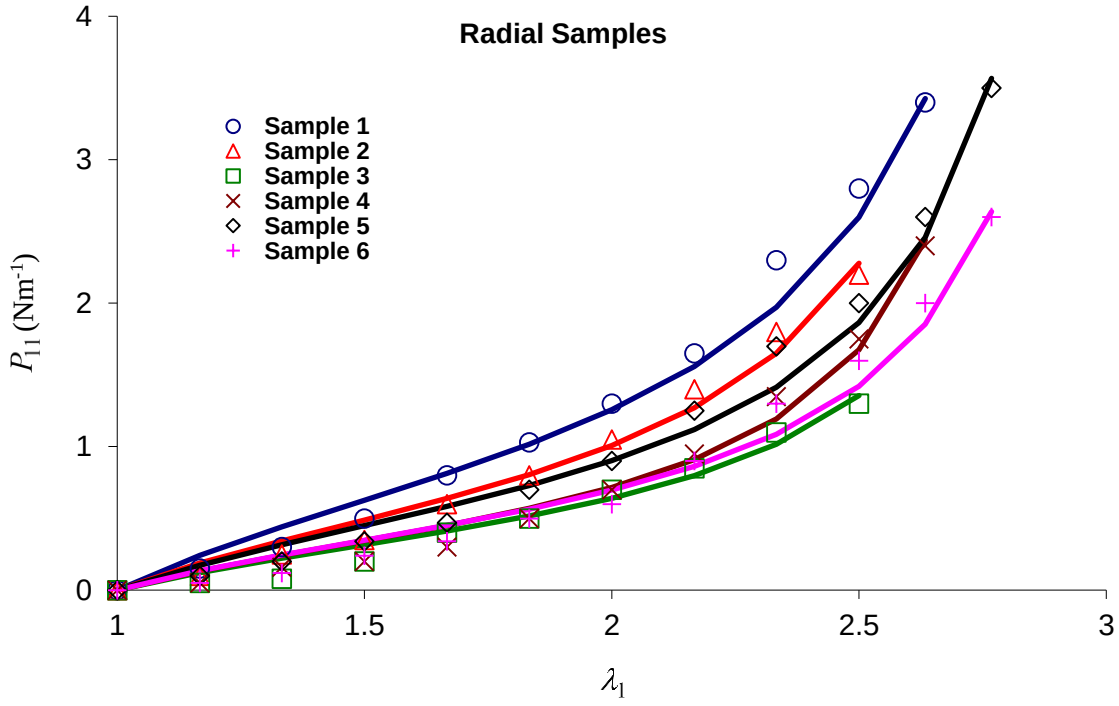
Radial Samples
P_{11} (Nm^{-1})
λ_1
0
1
2
3
4
1
1.5
2
2.5
3
Sample 1
Sample 2
Sample 3
Sample 4
Sample 5
Sample 6

Figure 3

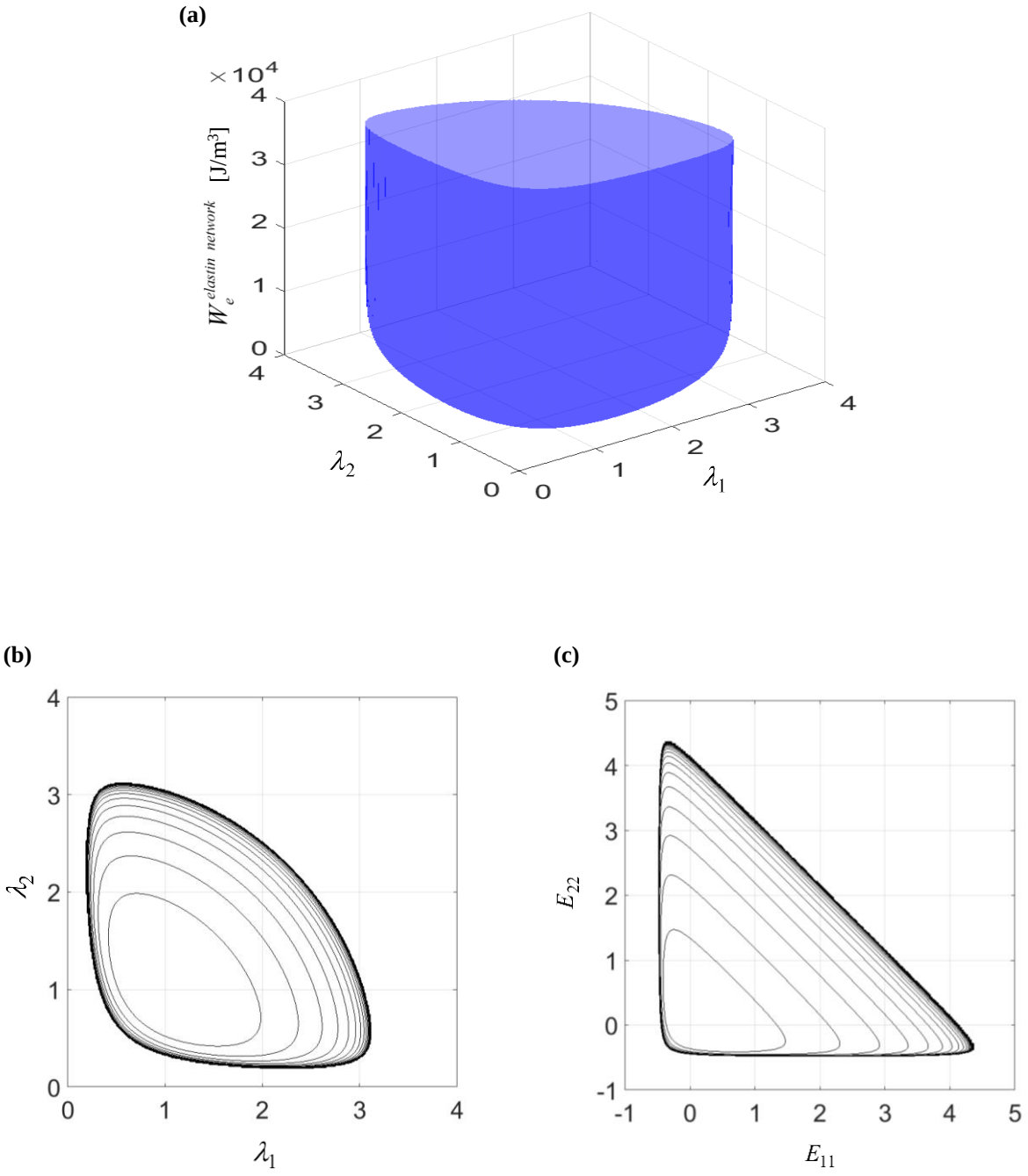
(a)
$\times 10^4$
$W_e^{elastin\ network}$ [J/m^3]
λ_2
λ_1
(b)
λ_2
λ_1
(c)
E_{22}
E_{11}

Figure 4

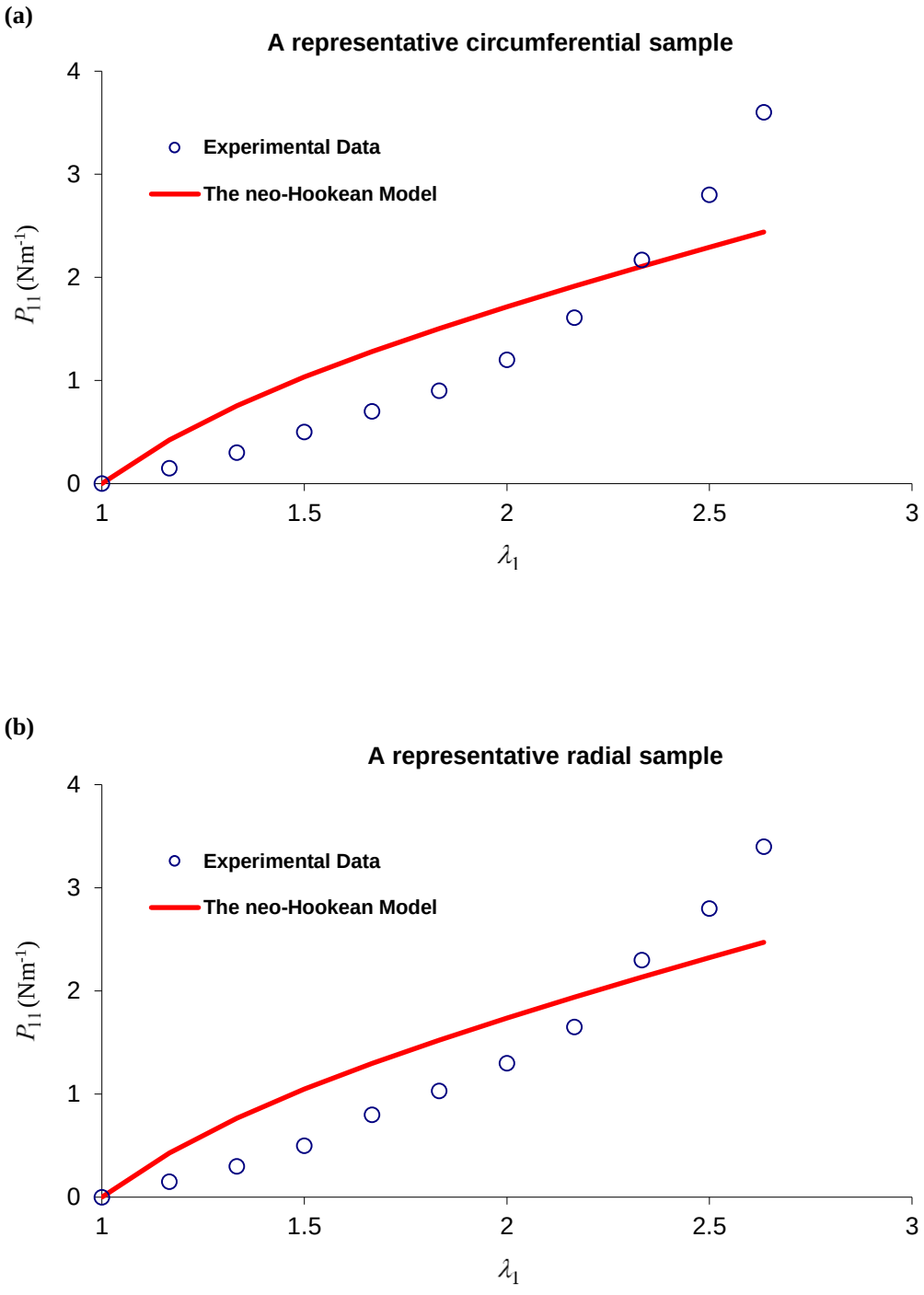
(a)
A representative circumferential sample
Experimental Data
The neo-Hookean Model
P_{11} (Nm^{-1})
λ_1
0
1
2
3
4
1
1.5
2
2.5
3
(b)
A representative radial sample
Experimental Data
The neo-Hookean Model
P_{11} (Nm^{-1})
λ_1
0
1
2
3
4
1
1.5
2
2.5
3

Figure 5

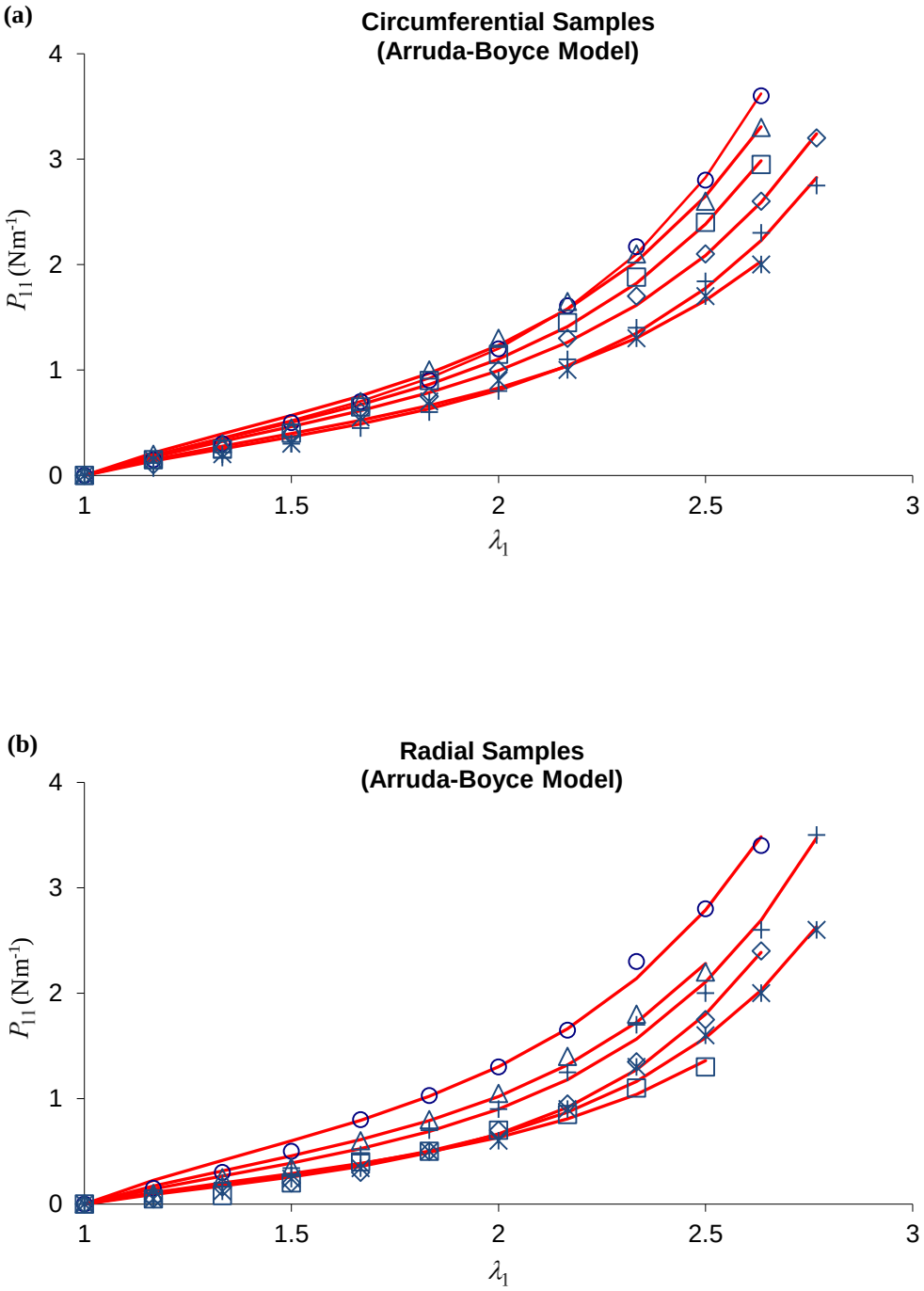
(a)
Circumferential Samples
(Arruda-Boyce Model)
P_{11} (Nm^{-1})
λ_1
0
1
2
3
4
1
1.5
2
2.5
3
(b)
Radial Samples
(Arruda-Boyce Model)
P_{11} (Nm^{-1})
λ_1
0
1
2
3
4
1
1.5
2
2.5
3

Figure 6

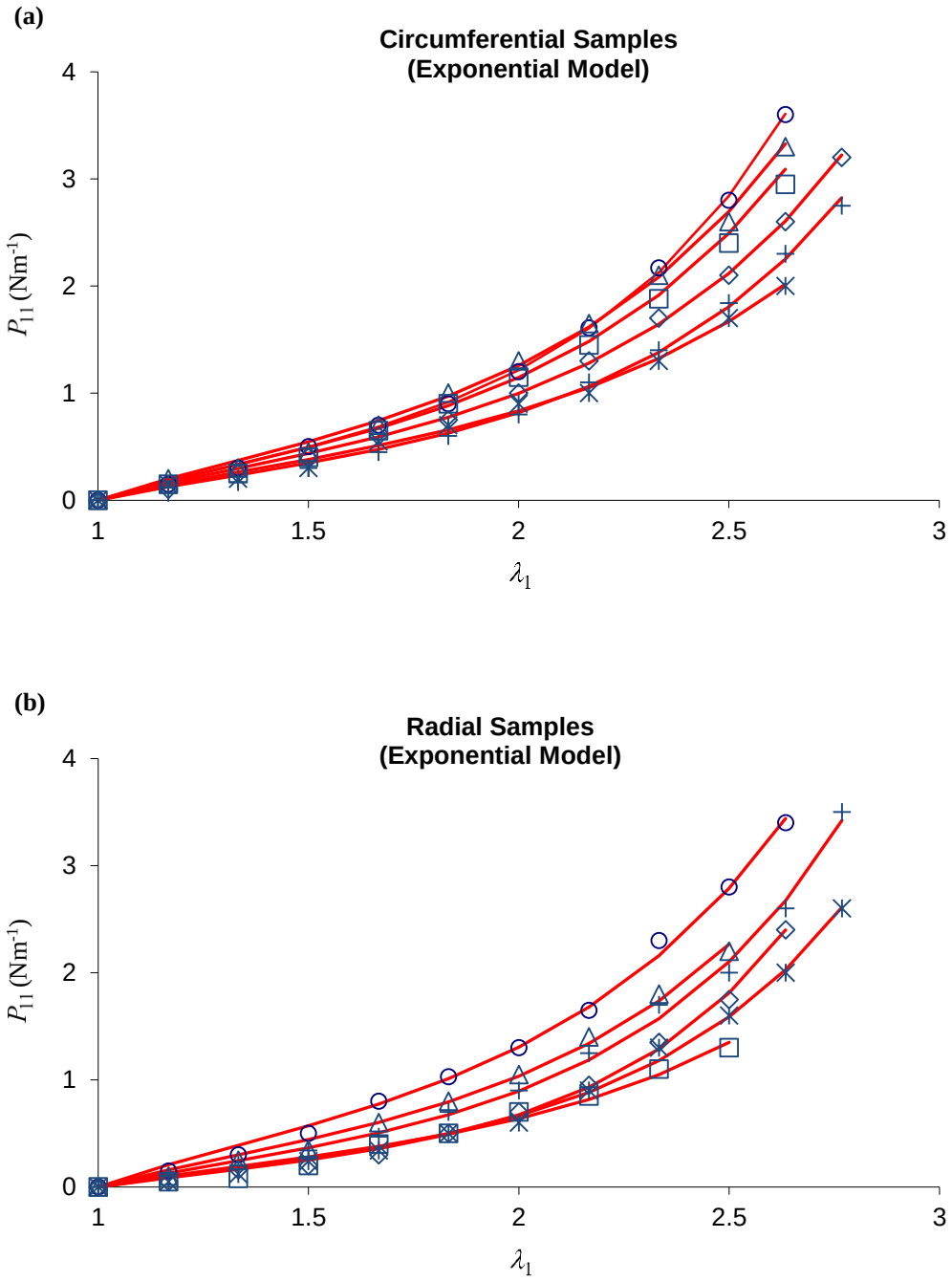
(a)
Circumferential Samples
(Exponential Model)
P_{11} (Nm^{-1})
λ_1
0
1
2
3
4
1
1.5
2
2.5
3
(b)
Radial Samples
(Exponential Model)
P_{11} (Nm^{-1})
λ_1
0
1
2
3
4
1
1.5
2
2.5
3

Figure 7

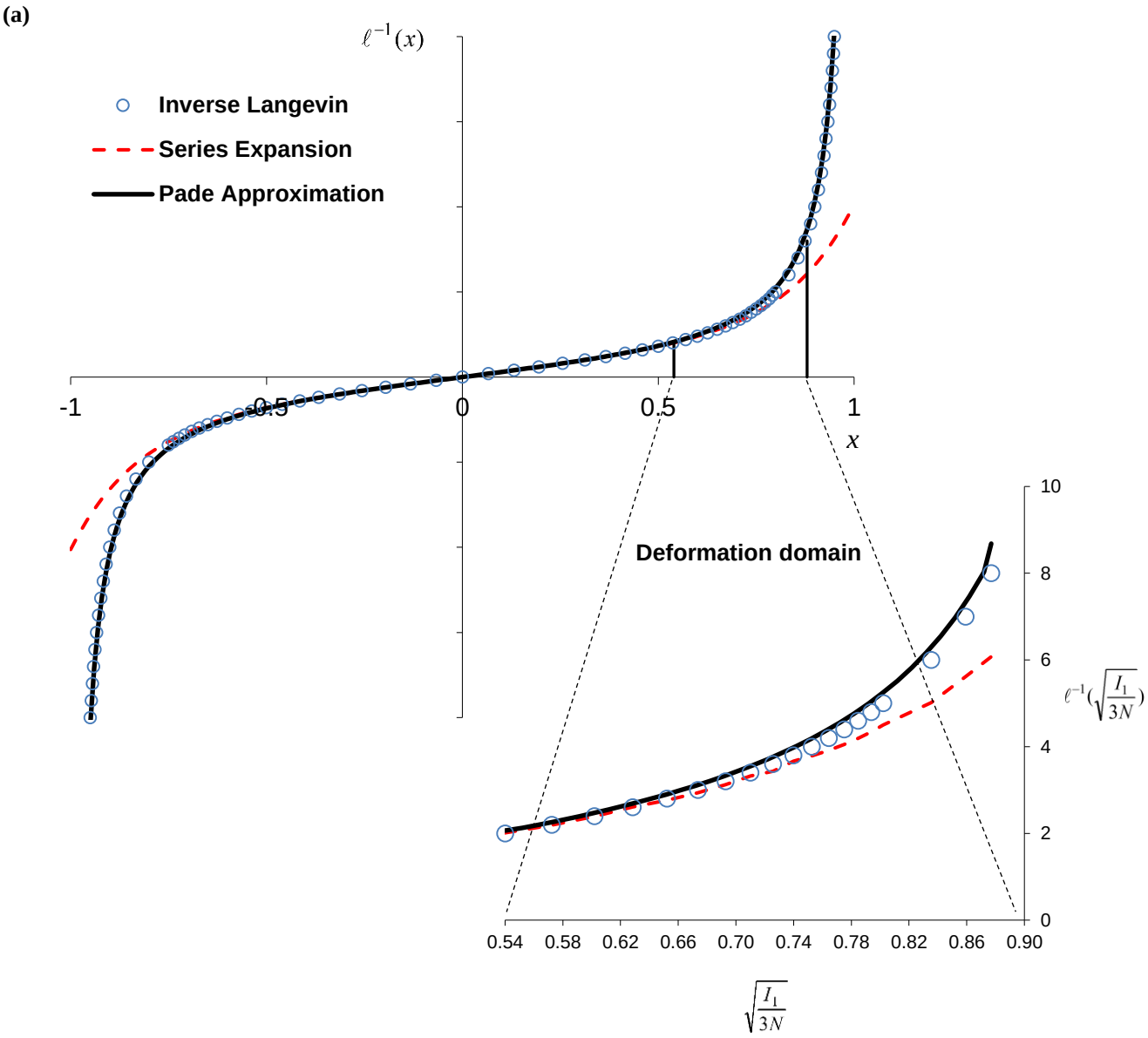
(a)
$\ell^{-1}(x)$
Inverse Langevin
Series Expansion
Pade Approximation
-1
-0.5
0
0.5
1
x
Deformation domain
0.54
0.58
0.62
0.66
0.70
0.74
0.78
0.82
0.86
0.90
$\sqrt{\frac{I_1}{3N}}$
$\ell^{-1}(\sqrt{\frac{I_1}{3N}})$
0
2
4
6
8
10

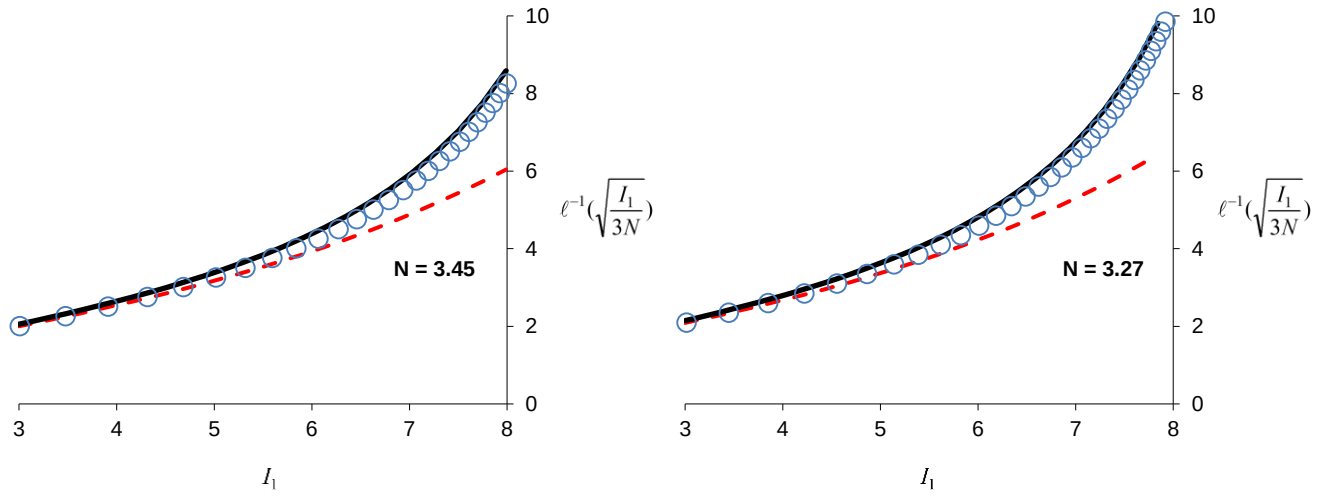
(b)
N = 3.45
N = 3.27
$\ell^{-1}(\sqrt{\frac{I_1}{3N}})$
3
4
5
6
7
8
I_1
0
2
4
6
8
10